Physics 256
Natural Computation & Self-Organization
Coupled-Oscillator Models: State-Space & Dynamics

Chris Warner
Biophysics Graduate Group
Redwood Center for Theoretical Neuroscience
University of California, Berkeley
cwarner@berkeley.edu

June 11, 2013

Abstract

Objects and systems at all scales operate by a mix of internal impulsion and external influence. This phenomenon, ubiquitous and accurately modeled by simple systems of coupled oscillators, are observed in systems of elementary subatomic particle, biological populational dynamics and interactions of heavenly bodies on an astronomical scale. Despite the simplicity of coupled oscillator models like Kuramoto's and the Dripping Handrail, they contain rich behavior such as phase transitions and harbor computational capabilities. The combination of simplicity, leading to mathematical tractability, and rich behavior is why coupled oscillator systems are so heavily studied. We study the dynamics and information storage capacity of a small, simple system of coupled oscillators - with ultimate goals of elucidating neural oscillatory behavior and investigating the computational benefits that such oscillatory behavior might engender. We map out the phase space and dynamics of a single discrete-time, discrete space Dripping Handrail (DH) oscillator system and examine what additional complexities arise when two DH oscillators are coupled together. We investigate interactions between natural frequencies, coupling strengths, coherence, coupled frequencies and relative phase of a two oscillator system. We also discuss the application of these ideas to a 3 DH oscillator system and the additional considerations for systems of 3+ oscillators.

I. Introduction

Motivation

Rhythmic or oscillatory behavior is observed in natural phenomena such as heart pacemaker cells [], central pattern generators for locomotion [], synchronization of metronomes [], and fireflies [], flocking and schooling behavior of birds and fish [], and most interestingly neural circuits []. With oscillatory phenomena all around us in nature, there is great need to analyze and understand such behavior. Often large systems of interacting individuals are analyzed with techniques from mean field theory, where the effect of all the other individuals on any given individual is approximated by a single averaged effect, thus reducing a many-body problem to a one-body problem []. While these powerful techniques yield qualitative behavior (and one could argue understanding) of complex systems such as phase transitions or the bifurcation from disorder to a synchronized state, they do not allow the observer to peer down beneath the vale of the average behavior of the system or to understand the individual dynamics and influences between small numbers of individual units. Such techniques when used in isolation may rob the investigator of key insight and intuition and may actually obfuscate the complex and rich dynamics of these systems beyond phase transitions.

Impact

The potential impact of new detailed study of small systems of coupled oscillators can be far-reaching. We have specific interest in their application to problems of Image Segmentation & Associative Memory, both of which require variable coupling between units for interesting computation to be performed. Mean field approaches applied to large systems, in order to maintain their mathematical tractability have restricted systems to uniform, undirected coupling. As a result, their activity is either completely unsynchronized, or in varying degrees of synchronization where oscillators with commensurate natural frequencies cluster first just beyond the bifurcation point. The result applied to either of the above problems is uninteresting. In order to segment an image into multiple pieces or categorize elements as belonging to a specific memory (as in a Hopfield Network), it is necessary to have links between some elements stronger than others so that information propagates through the network in useful (i.e., non-uniform) directions.

Detailed coupled-oscillator model analysis can be used to investigate behavior where relatively small neighborhoods of densely connected clusters within larger networks dominate local activity. This network topology is highly relevant in many applications. In animal flocking behavior, **Bialek et al. ??** showed in [] that the beautifully complex emergent behavior starling flocks can be qualitatively reproduced in models where each bird influenced by just 7 of its nearest neighbors, regardless of their physical distance. Human social networks have similar topological structure, where most people are strongly connected to few others (when considering the size of the whole network) who are likely strongly connect to eachother. Similarly, each neuron in the brain makes an average of just 1000 connections to other neurons out of the $\mathcal{O}$(100 billion) neurons in the human brain []. These local interactions between relatively small clusters neurons

result in spectrally-diverse, temporally-dynamic oscillatory patterns on different spatial scales across and within different brain regions. A detailed understanding of local interaction and dynamics in such networks would be a large step in the direction of a better understanding of information spread throughout these networks on the large scale.

Outline

In section II, we will discuss the nature and role of oscillatory dynamics in neural circuits, as well as non-oscillatory models that have been devised to implement Associative Memory and Image Segmentation. Section III contains a detailed description of the two coupled-oscillator models investigated, the Dripping Handrail and the Kuromoto Model. In section IV, we discuss the specific perturbations we made to the single oscillator and two oscillator systems and the logic behind out investigations. Section IV also contains a discussion of the synchronization metrics we report in the results section. In section V and VI, we report the results of our simulations and discuss implications and further applications.

II. Background

Neural Oscillations

Neural Oscillations have been measured using Electrocorticography (ECoG), Electroencephalography (EEG) and single electrodes implanted in neural tissue. They occur across a wide range of frequencies and are found both localized within particular brain regions as well as across brain regions. Alpha waves (8-12Hz) dominate in the Occipital lobe of the brain (the house of the cortical visual system) and their same frequency counterpart, Mu waves, exist in motor cortex. Activity is attenuated during active looking and motion, respectively. Beta rhythms (12-30Hz) are associated with active, busy, or anxious thinking and active concentration []. Delta waves (0-4Hz) are active in deep sleep []. Theta waves (6-10Hz) are active in Hippocampus and have been shown to encode localization of an animal in the environment [1] [2]. Gamma oscillations (25-100Hz) have been linked to consciousness [3] and visual attention [4] [5]. While their existence is well established, the utility of neural oscillations for coding and computation is a contraversial topic. Simulated networks of connected inhibitory and excitatory populations of recurrently connected spiking neurons (E-I Networks) have been shown to exhibit oscillatory behaviour [16] and some researchers consider oscillations as epiphenomena which arise from these networks.

Conversely, neural oscillatory activity is posited to be used in feature binding [6] [7] [8], temporal coding [12] [13] (in complement to the well established rate code held as the format of the neural code since 1926 [14] [15]) and communication on different scales [9] [10] [11]. The well known "binding problem" addresses the lack of explanation of how brains segregate elements in complex patterns of sensory input so that they are not muddled together, but allocated to discrete and relevant inputs from the external environment. Neural oscillation have been argued as a mechanism to solve the binding problem because they allow for attributes belonging to different objects to be segregated by the relation-

ship of spikes to the underlying phase of the local field potential (LFP). The binding by coherence theory is a specific instance of the temporal coding hypothesis, which states that the specific timing of spikes within spike trains encodes relevant information about stimulus and experience. The temporal code is argued to exist alongside and in addition to the rate code, which has been shown to encode localized features of stimulus in the average firing rate of neurons in chosen time windows.

Beyond encoding relevant information about stimulus, oscillations are thought to play a key role in communication between neurons and neuronal populations in the brain. The "Communication-Through-Coherence" hypothesis states that dynamic functional links are quickly established and abolished between neuronal ensembles and brain regions by phase coherence of oscillations between units. Specifically, neurons in A communicate more effectively with B if their LFP oscillations are in phase because neurons in B are closer to firing thresholds when spikes from A arrive. Conversely, the functional link between A and C is "cut" if their oscillations are out of phase with one another. Similarly, according to a theory known as "Cross Frequency Coupling", communication between brain regions dominated by different oscillatory frequencies can be achieved when a harmonic relationship and phase locking exists between those oscillations. Through this mechanism, lower frequency oscillations such as Alpha and Beta (which often dominate higher regions in the neural hierarchy) can entrain higher frequency ones (prominent in lower regions closer to the sensory periphery), effectively opening a communication channel for the implementation of top-down control.

Hopfield Associative Memory Network

In 1982, J.J. Hopfield [17] [18] developed a neural network model for memory storage and retrieval. He extended the Ising model of ferromagnetization [19] to systems with all-to-all symmetric connectivity (non-sparse $\mathbf{W}$ with $W_{ij} = W_{ji}$) in binary or bipolar systems ($\mathbf{s} \in \{0, 1\}$ or $\{-1, 1\}$ respectively) and established network dynamics in which any input state converges to a fixed point attractor by descending a quadratic energy landscape or a Lyapunov function.

$$E(s) = -\frac{1}{2}\sum_{ij} W_{ij} s_i s_j - \sum_i b_i s_i \tag{1}$$

Each update of the state vector $\mathbf{s}$ is guaranteed to not increase the energy [17]. The result is that a Hopfield network will find the local minimum that is closest to the starting state (measured in Hamming distance, or number of bit flips difference). The network is constructed in such a way that local minima correspond to stored patterns.

The update rule for each unit determines whether it remains in its current state or flips to the opposite available binary state.

$$s_i = sgn(\sum_{j \neq i} W_{ij} s_j - b_i). \tag{2}$$

Intuitively, the above equation says that each individual neuron decides its next state by

measuring the linear combination of all its inputs (first term) and comparing that sum to its threshold (b_i). The signum function (sgn) implements a hard-threshold or step function that makes the dynamics of the system deterministic. If the sum of input "voltages" (in a physiological neuron interpretation) passes threshold, the neuron will fire, taking a value of +1. If it does not, the neuron will be inactive, taking a value of -1. Network dynamics that adjust the **s** values given a fixed weights matrix **W** are implemented using eq. 2, with both parallel (all neurons at once) and asynchronous (one at a time and random order) update procedures.

Hopfield networks, also called autoassociative networks, have been predominantly used to store and retrieve input patterns and can do denoising. Learning patterns is analogous to digging out minima in the energy landscape. The Outer Product Rule implements Hebbian learning to store memories, or patterns, in the weights of the **W** matrix. It is given by:

$$\mathbf{W} = \sum_k \mathbf{s}_k^T \mathbf{s}_k - \mathbf{I}. \tag{3}$$

where k is the number of patterns to store in the network, T is the vector transpose operator and I is the identity matrix, subtracted off because there is explicitly no self interactions in the Hopfield model. The Outer Product Rule can store $\mathcal{O}(\mathrm{N}/(4\ln(\mathrm{N})))$ unique uncorrelated patterns in the weights of a network consisting of N neurons [**?**]. Other learning rules such as the Perceptron Learning Rule can store more patterns, but are beyond the scope of this work. Hopfield significantly advanced the Ising model by providing a Hebbian learning rule for the weights in eq. 3 and network dynamics in eq. 2 that guaranteed convergence to a local minima, corresponding to a stored pattern. One drawback however of Hopfield networks is that they also store spurrious minima corresponding to linear combinations of stored patterns. We postulate (section VI) that the inclusion of oscillatory dynamics, analogous to the Dynamical Systems models discussed in section III may untangle multiple patterns from one another within these spurrious minima by separating them in phase of oscillation.

Spectral Clustering & Image Segmentation

Spectral Graph Theory (SGT) is the study of properties of a graph in relationship to the eigenvalues and eigenvectors of matrices associated to the graph [20] [21]. It is closely related to Principle Components Analysis (PCA), which elucidates the dimensional structure of a distribution of data by examining the eigenspectrum of the data's covariance matrix [22] [23]. In both PCA and the spectral decomposition of a graph, the eigenvectors with the largest corresponding eigenvalues capture the most salient features of the underlying data/graph. The connection between the eigenspectrum of a graph and the dynamics of an associated coupled oscillator system is less clear, but it is reasonable to think of the eigenspectrum of the graph as the steady state solution to the dynamics of the coupled oscillator system with the largest eigenvectors containing the most prominent modes of oscillation.

In past research on image segmentation and graph partitioning using SGT, the graph has been constructed in one of several more-or-less heuristic ways. First the Adjacency or Similarity of graph elements is determined to be a Gaussian function (with variance σ) of some properties of those elements:

$$\mathbf{A}_{ij} = e^{-\frac{(Z_i - Z_j)^2}{2\sigma^2}} \tag{4}$$

More concretely, Z_i and Z_j can be greyscale intensity values at pixels i and j, the activation of oriented localized filter bank elements, or similarity of answers to questions asked on a questionaire for a dating website, perhaps. The first and simplest approach, known as Average Association, simply calculates the eigenspectrum of the Adjacency matrix [24]. The Adjacency matrix is symmetric with zero diagonal because connections are undirected and self-connections do not exist.

The Graph Laplacian $\mathbf{L}$ additionally takes into account the degree of each node in the graph by adding its value to the negative of the Adjacency matrix.

$$\mathbf{L} = \mathbf{D} - \mathbf{A} \tag{5}$$

The Degree matrix $\mathbf{D}$ is is a diagonal matrix where each entry along the diagonal is just the row (or equivalently column) sums of the Adjacency matrix. The Graph Laplacian has very interesting connections to random walks on graphs [25], electrical potential theory [26] [32], and mass-spring systems by the duality between physical oscillators and electrical circuits. The normalized Graph Laplacian was used in the successful and highly cited N-cut algorithm of Shi & Malik [27].

The Modularity method [28] [29] [30] [31] has been used successfully for cluster finding in social networks. Similar to the Graph Laplacian, it takes into account the degrees of (or incidence into) nodes, but it does so in order to compute a "Null Model" that is subtracted from the Adjacency matrix. The Null Model $\mathbf{N}$ quantifies the expected strength of connection between nodes i and j. It is calculated by a multiplicative relation of the degrees of nodes i and j normalized by the total degree of all nodes in the graph. Intuitively, we expect a strong weight to exist between nodes i and j in the Modularity matrix $\mathbf{M}$ if they both have large numbers of strong connections compared to the number and strength of connections in the graph on the whole. That is,

$$\mathbf{M} = \mathbf{A} - \mathbf{N}, \quad \text{where} \quad \mathbf{N} = \frac{\mathbf{D}^T\mathbf{D}}{\sum_{ij}\mathbf{A}} \tag{6}$$

Once the Modularity matrix is calculated, its eigenspectrum is calculated, with the largest eigenvector leading to a salient bipartition of the graph. Further (2+ segments) partitions of a graph are possible by iterating the algorithm on subgraphs or by considering more than just the largest eigenvector. As far as we know, the Modularity method has only been applied to networks with no underlying topological structure. It requires a small extension to the null model in order to apply Modularity methods to images for the task of image segmentation. We are currently investigating this application of the method.

III. Dynamical System

As discussed in the above section on Spectral Graph Theory, the eigenspectrum may be an approximation of or a proxy for the full dynamics of the coupled oscillator (or electrical network) system associated with a given graph. In order to extract structure on different scales in an image, an algorithm which implements SGT must use multiple eigenvectors or an iterative bipartitioning scheme along with arbitrarily chosen threshold values. Far more neurologically plausible, a dynamical system model could hypothetically extract hierarchical structure by coding it in either phase of oscillation or temporal evolution of the system (perhaps coding gross, large-scale structure and refining the image to smaller details based up on time allowed and attentional cues). In order to investigate the dynamics of coupled oscillator systems and gain intuition, we study two systems below.

Kuramoto Phase Oscillator Model

The Kuramoto model, introduced by Yoshiki Kuramoto in 1984 [33] [34], consists of a mathematically tractable, mean field model of a system of N coupled oscillators with a uniform coupling constant K between all oscillators and a unimodal Gaussian natural frequency distribution ω,

$$\frac{\delta\theta_i}{\delta t} = \omega_i + \zeta_i + \frac{K}{N}\sum_{j=1}^{N} sin(\theta_j - \theta_i) \tag{7}$$

where ζ is a small Gaussian noise term. This simple discrete space, continuous time model which considers only phase of oscillators is interesting because it exhibits a phase transition at a critical parameter setting, known as a bifurcation. Equation 7 describes a balance between two opposing forces. The magnitude of spread of the natural frequency distribution mediates the dispersive force between oscillators that keeps them from locking into a similar phase of oscillation. Opposingly, the strength of the coupling constant modulates an agglomerative force imposed by the sine function that tries to cluster oscillators into the same phase. For a given natural frequency distribution, there is a critical coupling parameter value K_c at which oscillators begin to lock into the same phase. Below K_c, the system is in a disordered state with the phase of oscillators evenly spread around the unit circle. Nearby the bifurcation parameter setting, we witness oscillators with natural frequency near the center of the normal distribution locking while ones in the tails of the distribution remain disordered. As K is increased further beyond K_c, we find more and more oscillators locking until eventually, for K large enough, the system falls into the fully synchronized state with all oscillators evolving at the same phase and mean frequency regardless of their natural frequency.

Dripping Handrail Circle Map

The Dripping Handrail (DHR) Circle Map is a discrete space, discrete time dynamical system model first introduced to model accretion phenomena in astronomical systems [35] [36]. The DHR model is similar to the Kuramoto model in that it exhibits phase transition in the mean field regime when the ratio of coupling parameter to natural frequency

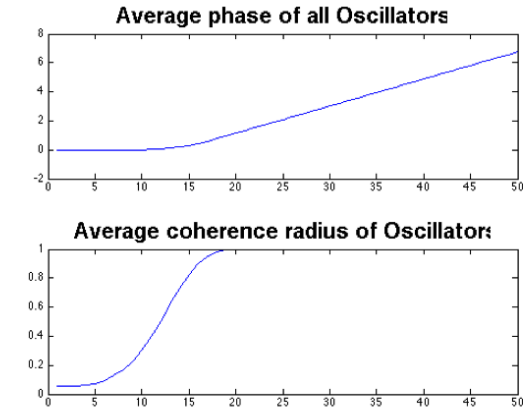

Figure 1: Phase Distribution and Coherence Radius time evolution of Kuramoto Coupled Oscillator System with $K > K_c$

distribution (c/σ_w) is sufficiently large. The dynamic equation for the time evolution of the DHR system is

$$x_{t+1}^i = \omega^i + sx_t^i + c(x_t^{i-1} + x_t^{i+1})(mod1) \tag{8}$$

where $\omega^i \in [0, 1]$ is the natural frequency of oscillator i, parameter s is the slope of the map function ($0 <$ s $\ll 1$) and $c \in [0, 1]$ is the coupling constant between oscillators. The indices i denote the discrete spatial location of the oscillator and t denote the discrete timestep. The dynamics of a single dripping handrail ramp up at a constant linear rate (determined by ω for s $\ll 1$) and then reset back to zero by the (mod 1) function. For larger s, the dynamics become a non-linear, exponential growth function that gets reset to zero when it reaches 1. In the original model, c is a constant and only nearest neighbors at lattice sites (i-1) and (i+1) are considered linked to oscillator i. Like the Kuramoto model, Dripping Handrail oscillators when coupled together exhibit a phase transition at a critical parameter value, or a bifurcation point.

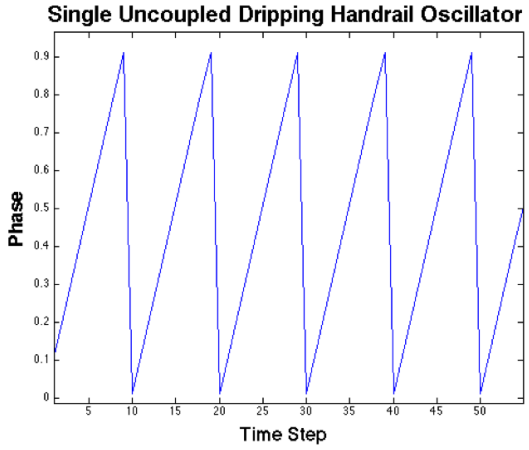

Figure 2: Dynamics of a single, uncoupled Dripping Handrail Circle Map

IV. Methods

Our attempt to gain insight into they dynamics of and map out the state space of coupled dripping handrail circle maps began with a detailed analysis of the state space of a single uncoupled handrail (for c=0). The exploration of natural frequency, numerically computed using Fourier analysis yielded no dependence on the s parameter for small enough parameter values. For s parameter values larger than approximately 10^{-4}, the natural frequency of a single DHR oscillator deviated from the analytical natural frequency. After the initial exploration, we chose a value of $s = 10^{-7}$. In figure 3, we show the difference between natural frequencies of two uncoupled DHR maps for different settings of each map's ω parameter value.

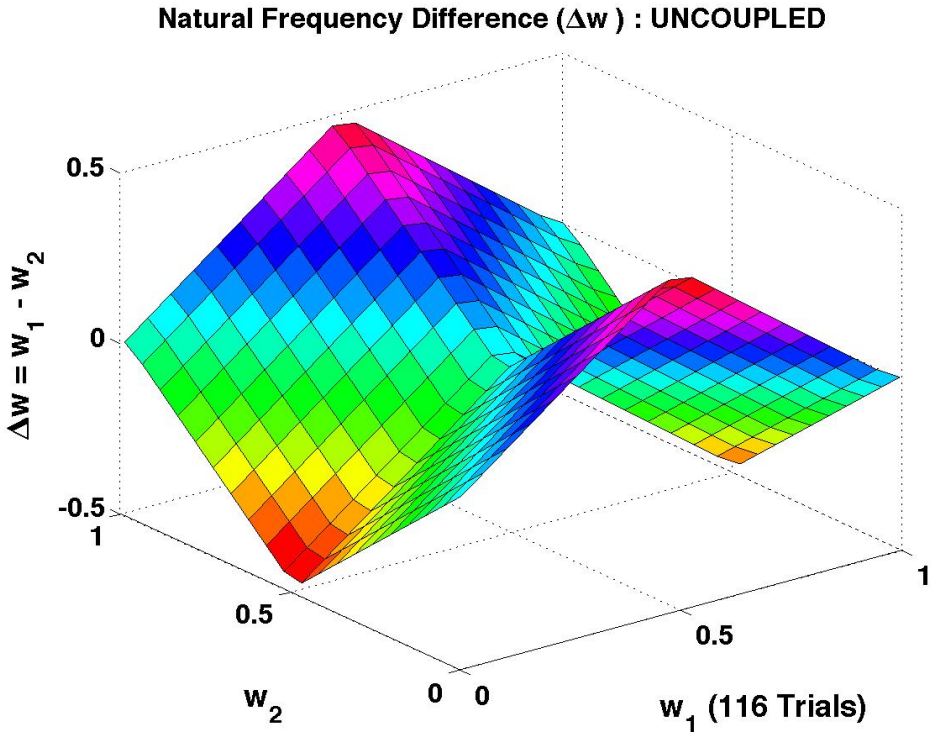

Figure 3: Natural Frequency Difference between 2 uncoupled oscillators

After mapping out the statespace of single DHR, we investigated a system of two coupled DHR oscillators varying 4 parameters $(\omega_1, \omega_2, c_1, c_2)$ independently. We ran 116 randomly initialized tests each one sampling 20 ω parameter values evenly spaced between 0 and 1 for each oscillaor independently and 11 coupling parameter values at increments of 0.1 between 0 and 1 for each coupling separately. For each individual parameter setting, we initialized the simulation and allowed it to run for 2000 timesteps, recording the measurements quantities for analysis. This paradigm allows us to explore a whole class of 2 oscillator systems that display a range of interesting behavior and scale up to very different systems with the addition of more oscillators. By varying the ω parameters, we could explore the entire space of natural frequency relationships between oscillators 1 and 2. By varying the c parameters together, we could explore the space of undirected (meaning reciprocally connected) oscillator systems. By varying them separately, we could explore

dynamics in directed networks (a phenomenon that will increase in complexity and interest when networks of 3+ oscillators will be considered.

In order to quantify the synchronization of each system, we calculated three values separately, the dominant coupled frequency for each oscillator, the coherence radius for the system and the phase difference between the two oscillators. We calculate the coupled frequency of each oscillator by taking the discrete Fourier transform of its position as a function of time, shown in figure 2 and taking the frequency of the dominant peak (away from the DC peak at 0Hz. We then report the coupled frequencies of each oscillator individually. If they locked due to coupling, we expect that their coupled frequencies should match. Upon thought about real oscillator systems, we discover something lacking in the simplistic difference in frequency measure. There is a possibility of oscillators locking when one frequency is a harmonic mulitple (i.e., integer multiple) of the other. It seems that a better measure to capture this phenomenon would be a difference of the modulus of the ratios of oscillators, see figure 4. We calculate the modulus-1 of the ratios of ω_1/ω_2 and ω_1/ω_2 and plot the values on a discrete colormap indicating the percent distance of the ratio from an integer one. White means exactly harmonic and black means more that 10

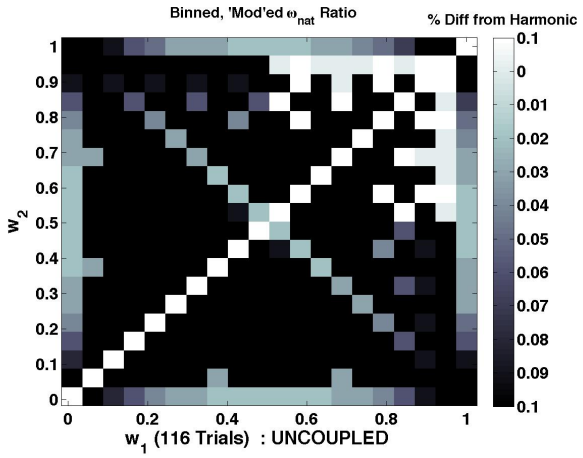

Figure 4: Natural Frequency Difference between 2 uncoupled oscillators

Since it is conceivable that two oscillators could be locked in frequency, but at the same time entirely incoherent - that is, locked in antiphase, we also calculate the coherence radius. At each timepoint, the Coherence Radius R_c is calculated as

$$R_c(t) = \sqrt{< cos(\theta) >^2 + < sin(\theta) >^2} \tag{9}$$

where the $<.>$ notation denotes expected value or mean across oscillator population. In order to condense this T length vector into 2 scalar quantities, we take the mean and standard deviation of R_c. The motivation behind this simplifying transformation is that given a sequence long enough for oscillators to lock, their locked dynamics will dominate when timepoints are averaged over. Consequently, the mean R_c value will be large and the standard deviation will be small. Conversely, systems that do not lock will have a middling range average R_c value and a relatively large standard deviation. Systems that

stand on the border of punctuated coherence (locking and unlocking repeatedly) will have a large standard deviation as well. The measure unfortunately breaks down and fails to provide useful information about a system that has separate populations of oscillators locked into antiphase or into different phases around the unit circle. The coherence radius of two antiphase oscillator populations is exactly the same as a completely random distribution of oscillator phases.

Lastly, we calculate the mean and standard deviation on the phase difference between two oscillators to ascertain whether they are locked in a stable phase relationship whether that relationship is in-phase, anti-phase or 37° out of phase. This measure provides information where coherence radius fails. It also provides some information about the frequency relationship between oscillators - namely, if the standard deviation of difference in phase is zero, they must have the same frequency. It also, however, breaks down in the case of harmonic frequency relationships. In this case, it may be more informative to look at the distribution of phase relationships. It the distribution is multimodal, the number of peaks would tell the frequency relationship between oscillators. This measure also suffers from combinatorial explosion when you consider systems of many oscillators because a phase difference necessarily involves pairs of oscillators. In a system of N oscillators, you have $\binom{N}{2}$ pairs of phase differences. While they work well for the simple 2 oscillator systems considered within, our analysis techniques must be extended if they are to remain useful in the detailed analysis of general coupled oscillator systems.

V. Results

Though we have taken data for a wide range of parameter settings in two DHR oscillator systems, the limited amount of time alotted for the project limits the amount of analysis that we could do. Consequently, we looked at some "sanity check" measures that woul alert us to fundamental problems in our approach or the code and then some simpler parameter combinations. We set fixed undirected coupling ($c_1 = c_2$) while varying the natural frequency of oscillators separately. Also, we fixed natural frequencies and looked at the reliance of our three measured quantities (frequency, phase and coherence radius) for varying coupling parameters. We have not yet looked at directed (i.e., unequal) coupling between oscillators. Likewise, we have not sufficiently explored harmonic frequency interaction between oscillators.

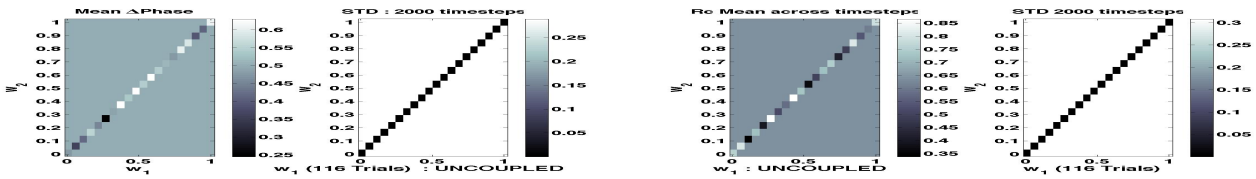

(a) Phase Difference (b) Coherence Radius

Figure 5: Uncoupled Oscillators with Natural Frequencies ω_1 and ω_2

Figure 5 displays the mean and standard deviation values both computed across the 2000 timesteps of each trial and then averaged across 116 trials. We can glean some

insights from these first few plots. Both phase difference and coherence radius are highly variable for two uncoupled oscillators with different natural frequencies. Conversely, both measures are highly structured (with zero variance) for uncoupled oscillators with the same natural frequency. Since they are uncoupled, the mean phase difference and R_c values are dependent on initial conditions of the simulation. The black diagonals in the standard deviation plots are most telling.

Next, we looked at difference in coupled frequencies for oscillators as a function of the natural frequency of each oscillator for fixed coupling parameter values. There is some very interesting structure in the series of plots in figure 6. The plot in a, where c=0, is a recapitulation of the plot in figure 3. Black areas in the plots show (ω_1, ω_2) parameter values that result in frequency locking for the given coupling parameter value. The off-diagonal black structure results from the circle map having identical natural frequencies for ω values symmetric about 0.5. That X structure migrates to smaller frequency values as the coupling parameter is increased and is replaced by a larger, noisier off-diagonal structure. When the coupling parameter goes to 1 in f, the basin of attraction of natural frequency parameter settings that result in frequency locking has increased. In figure 7, we plot the modulus-1 of the ratio of coupled frequencies to see the space in which cross-frequency coupling may work. Brighter spots denote harmonic structure in the coupled frequencies of the two oscillators.

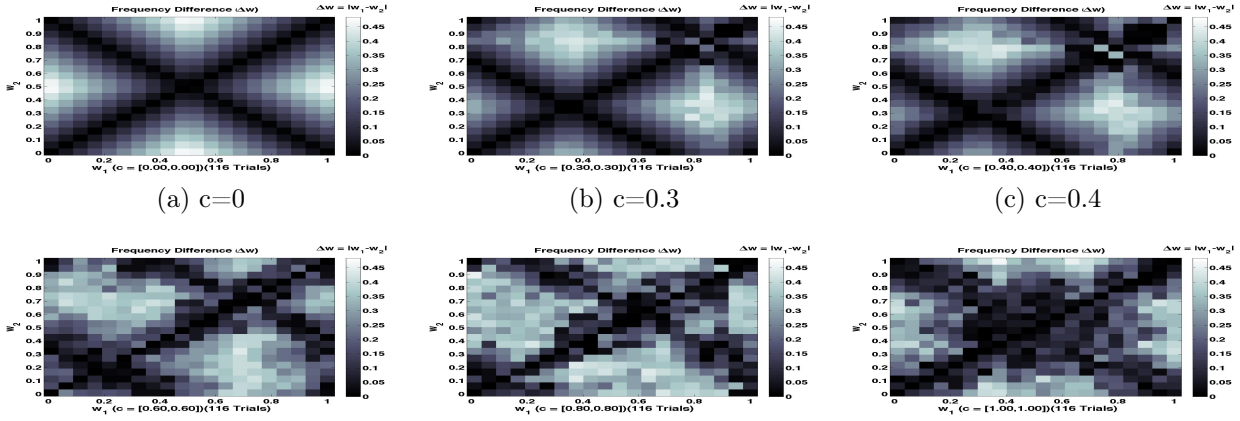

(a) c=0 (b) c=0.3 (c) c=0.4

(d) c=0.6 (e) c=0.8 (f) c=1

Figure 6: Coupled Frequency Differences $\Delta\omega = |\omega_1 = \omega_2|$

In figures 8 and 9, we see that there is very interesting structure that becomes more pronounced as coupling strength is increased. Uncoupled phase and R_c plots recapitulate figure 5. In these plots we can see the evolution of phase relationships and coherence radius as the coupling strength between oscillators is increased. In figure 8, we see that the oscillator with higher resonant frequency leads in phase the oscillator that it entrains. The phenomenon beomes more pronounced for stronger coupling. We also see in figure 9 that the coherence radius synchronization measure increases in intensity and size (essentially synching oscillators with more disparate natural frequencies) as the coupling parameter increases in strength.

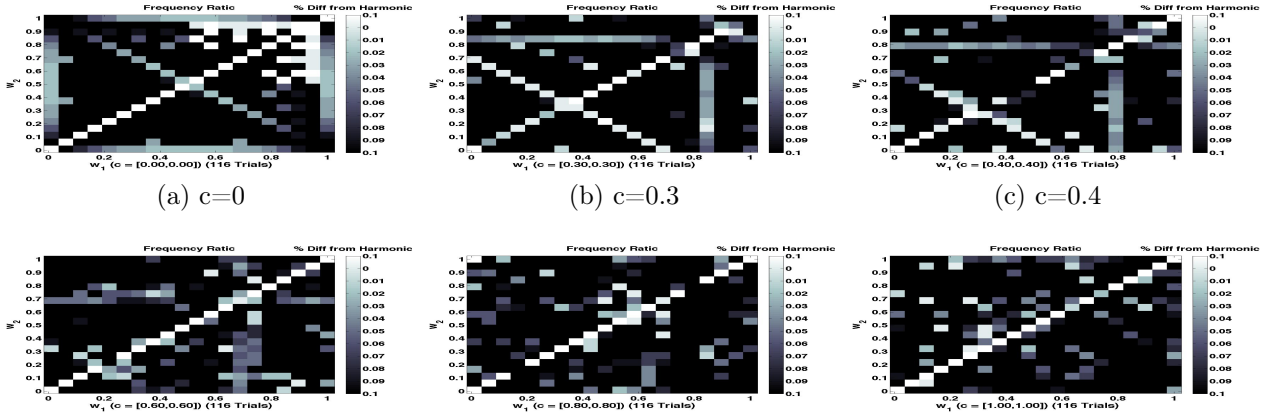

(a) c=0 (b) c=0.3 (c) c=0.4

(d) c=0.6 (e) c=0.8 (f) c=1

Figure 7: Coupled Frequency Ratios (Harmonic Frequency Structure)

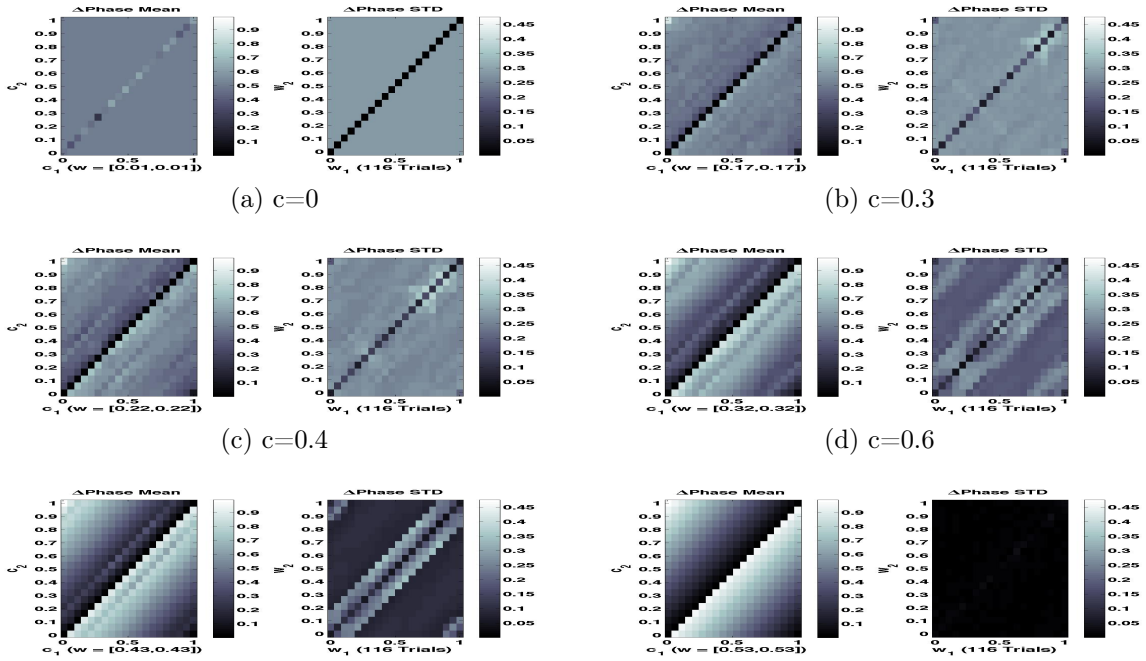

(a) c=0 (b) c=0.3

(c) c=0.4 (d) c=0.6

(e) c=0.8 (f) c=1

Figure 8: Coupled Oscillator Phase Relationship Statistics (Mean & STD)

VI. Discussion

While we have only just scratched the surface of what is possible and necessary in the detailed analysis of systems of coupled oscillators, we have found some interesting activity. The synchrony measures must be generalized and suitably adapted to convey useful information about larger more complex systems. We would immediately next like to look at a system of 3 coupled oscillators. This system has new and immensely interesting dynamics that would yield benefit if explored in detail We can investigate the tug-of-war system to analyze the synchronization of one intermediate oscillator when it is pulled by

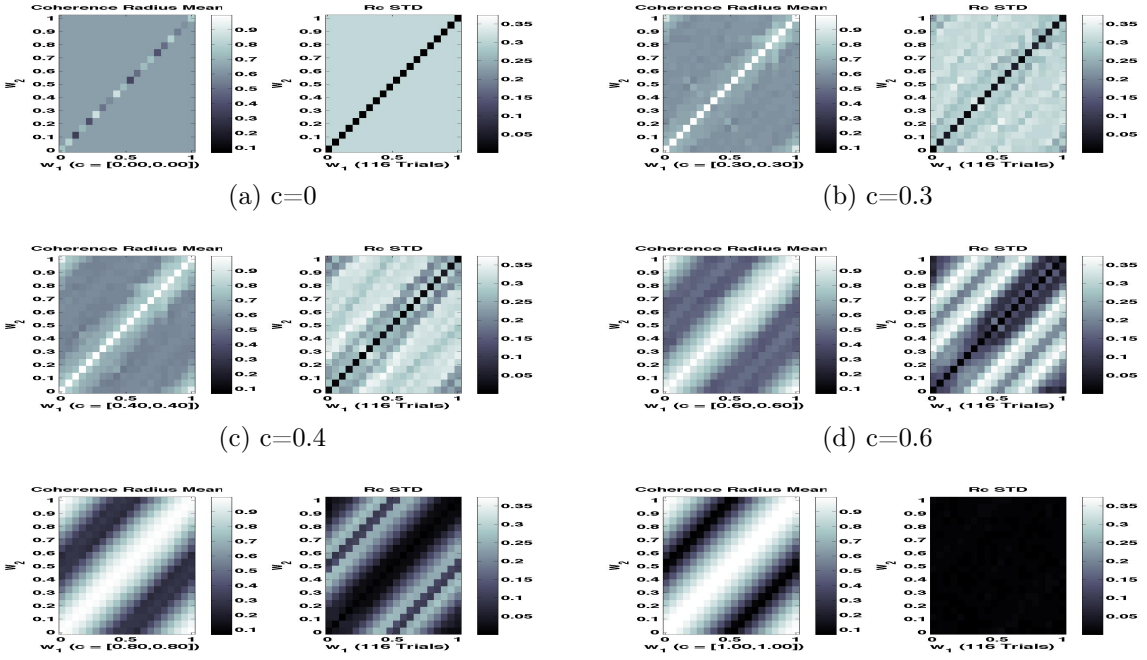

(a) c=0 (b) c=0.3

(c) c=0.4 (d) c=0.6

(e) c=0.8 (f) c=1

Figure 9: Growth of Basin of Coherence Radius with increased Coupling

two oscillators in opposing frequency directions with differing coupling strengths. We can look at the mob system and investigate how much more effective two locked oscillators are at recruiting other oscillators to their agglomeration. Finally, we can look at directed couplings with 3 oscillators where a loop of influence can be created and the system can enter some kind of ring-around-the-rosie dynamics.

I mentioned early in this work that variable coupling strengths are key to interesting computations being done in associative memory models and image segmentation algorithms. Starting from our small detailed analysis of the state space of these oscillatory systems, we would like to build up complexity to investigate the possibility of Hopfield-like associative memory storage in small systems of coupled oscillators (even 5 or 6 could yield some interesting and telling results). Perhaps such an oscillatory Hopfield network could separate stored patterns from one another into different phases of firing when presented with a mixture of stored patterns as input.

We would also like to investigate the usefulness of coupled oscillator models in applications of image segmentation. We postulate that the oscillatory dynamics of a properly primed connectivity network could segment images into salient regions by phase of oscillation. We propose this hypothesis as a method by which coarse segmentation of images can occur even as low down in the visual processing chain as retina. Gamma oscillations in retina, perhaps caused by the interaction of excitatory Rods/Cones & Bipolar cells with inhibitory Amacrine & Horizontal cells, may mediate this low level computation and processing of visual input by giving individual neurons temporal texture for the individual spikes they fire. In short, where a neuron lays down a spike in relation to the underlying retinal gamma oscillations can link sensory inputs eminating from a single external cause.

It is the larger goal of this investigation to understand how such a coding scheme could function and to build a model of its operation.

References

[1] G. Buzsáki, *Theta oscillations in the hippocampus*, Neuron 33.3 (2002): 325-340.

[2] N. Burgess, *Grid cells and theta as oscillatory interference: theory and predictions*, Hippocampus 18.12 (2008): 1157-1174.

[3] F. Crick, C. Koch, *Towards a neurobiological theory of consciousness*, Seminars in the Neurosciences v.2, (1990b) 263-275

[4] K. Koepsell, F. Sommer. *Information transmission in oscillatory neural activity*, Biological cybernetics 99.4-5 (2008): 403-416.

[5] R. Eckhorn, H. Reitboeck, et al. *Feature linking via stimulus-evoked oscillations: experimental results from cat visual cortex and functional implications from a network model*, Neural Networks, 1989. IJCNN., International Joint Conference on. IEEE, 1989.

[6] C. Von Der Malsburg, *The correlation theory of brain function*, Models of neural networks II: Temporal aspects of coding and information processing in biological systems (1981): 95-119.

[7] R. Eckhorn, et al. *Feature linking via synchronization among distributed assemblies: Simulations of results from cat visual cortex*, Neural Computation 2.3 (1990): 293-307.

[8] M. Usher, N. Donnelly. *Visual synchrony affects binding and segmentation in perception*, Nature 394.6689 (1998): 179-182.

[9] P. Fries, *A mechanism for cognitive dynamics: neuronal communication through neuronal coherence*, Trends in cognitive sciences 9.10 (2005): 474-480.

[10] R. Canolty, R. Knight. *The functional role of cross-frequency coupling*, Trends in cognitive sciences 14.11 (2010): 506.

[11] B. Voytek, R. Knight, et al., *Shifts in gamma phase–amplitude coupling frequency from theta to alpha over posterior cortex during visual tasks*, Frontiers in human neuroscience 4 (2010).

[12] F. Theunissen, J. Miller. *Temporal encoding in nervous systems: a rigorous definition*, Journal of computational neuroscience 2.2 (1995): 149-162.

[13] E. Ahissar, *Temporal-code to rate-code conversion by neuronal phase-locked loops*, Neural computation 10.3 (1998): 597-650.

[14] Adrian ED, Zotterman Y, *The impulses produced by sensory nerve endings: Part II: The response of a single end organ*, J Physiol (Lond.) 61 (1926) 151–171.

[15] D.H. Hubel, T.N. Wiesel. *Receptive fields, binocular interaction and functional architecture in the cat's visual cortex*, The Journal of physiology 160.1 (1962): 106.

[16] N. Brunel, X. Wang, *What determines the frequency of fast network oscillations with irregular neural discharges? I. Synaptic dynamics and excitation-inhibition balance*, Journal of Neurophysiology 90.1 (2003): 415-430.

[17] J.J. Hopfield, *Neural networks and physical systems with emergent collective computational abilities*, Proceedings of the national academy of sciences 79.8 (1982): 2554-2558.

[18] J.J. Hopfield, *Neurons with graded response have collective computational properties like those of two-state neurons*, Proceedings of the national academy of sciences 81.10 (1984): 3088-3092.

[19] E Ising, *A Contribution to the Theory of Ferromagnetism*, Zeitschrift für angewandte Mathematik und Physik 31.1 : 253-258. 1925

[20] F. Chung, *Spectral Graph Theory*, Conference Board of Mathematical Sciences Number 92, 1994

[21] U. von Luxburg, *A Tutorial on Spectral Clustering*, Statistics and Computing, 17 (4), 2007

[22] J. Schlens, *A Tutorial on Principal Components Analysis*, http://www.snl.salk.edu/ shlens/pca.pdf, 2009

[23] A. Azran, Z. Ghahramani, *Spectral methods for automatic multiscale data clustering*, Computer Vision and Pattern Recognition, 2006 IEEE Computer Society Conference on. Vol. 1. IEEE, 2006.

[24] S. Sarkar, K. Boyer, *Quantitative measures of change based on feature organization: Eigenvalues and eigenvectors*, Computer Vision and Pattern Recognition, 1996. Proceedings CVPR'96, 1996 IEEE Computer Society Conference on. IEEE, 1996.

[25] L. Grady, *Random walks for image segmentation*, Pattern Analysis and Machine Intelligence, IEEE Transactions on 28.11 (2006): 1768-1783.

[26] P. Doyle, J. Snell, *Random walks and electric networks* arXiv preprint math.PR/0001057 3 (2000).

[27] J. Shi, J. Malik, *Normalized Cuts and Image Segmentation*, IEEE TRANSACTIONS ON PATTERN ANALYSIS AND MACHINE INTELLIGENCE, VOL. 22, NO. 8, AUGUST 2000

[28] M.E.J. Newman, M.Girvan. *Finding and evaluating community structure in networks*, Physical review E 69.2 (2004): 026113.

[29] M.E.J. Newman, *Finding community structure in networks using the eigenvectors of matrices*, Phys. Rev. E 74, 036104 (2006)

[30] Palla, Gergely, et al. *Uncovering the overlapping community structure of complex networks in nature and society*, Nature 435.7043 (2005): 814-818.

[31] Danon, Leon, et al. *Comparing community structure identification*, Journal of Statistical Mechanics: Theory and Experiment 2005.09 (2005): P09008.

[32] N.Biggs, *Algebraic potential theory on graphs*, Bulletin of the London Mathematical Society 29.6 (1997): 641-682.

[33] Y. Kuramoto, *Cooperative Dynamics of Oscillator Community: A Study Based on Lattice of Rings*, Progress of Theoretical Physics Supplement 79.Supplement 1 (1984): 223-240.

[34] Y. Kuramoto, *Chemical oscillations, waves, and turbulence*, Courier Dover Publications, 2003.

[35] K. Young, J. Scargle, *The dripping handrail model: Transient chaos in accretion systems*. The Astrophysical Journal 468 (1996): 617.

[36] J. Crutchfield, K. Kaneko. *Are attractors relevant to turbulence?*, Physical review letters 60.26 (1988): 2715-2718.

[37] J Shlens, GD Field, JL Gauthier, MI Grivich, D Petrusca, A Sher, AM Litke EJ Chichilnisky *The Structure of Multi-Neuron Firing Patterns in Primate Retina*, Journal of Neuroscience, 26(32):8254–8266, 2006.

[38] E Schneidman, MJ Berry II, R Segev, W Bialek, *Weak pairwise correlations imply strongly correlated network states in a neural population*, Nature, 440:1007-1012, 2006.